Catalysis Letters 25 (1994) 115–126

Studies of carbon monoxide and hydrogen adsorption on nickel and cobalt foils aimed at gaining a better insight into the mechanism of hydrocarbon formation

A.L. Cabrera [1], W.H. Garrido M. and U.G. Volkmann

Facultad de Física, Pontificia Universidad Católica de Chile, Casilla 306, Santiago 11, Chile

Received 8 October 1993; accepted 14 December 1993

Systematic studies of adsorption of hydrogen and carbon monoxide on polycrystalline surfaces of nickel and cobalt have been carried out. The aim of these studies was to gain a better insight into the catalyzed formation of hydrocarbons from H_2–CO mixtures. We have studied the adsorption of these gases by means of thermal desorption spectroscopy (TDS) on nickel foils and powders. More recently, we have obtained desorption spectra of hydrogen adsorbed on cobalt foils and powders. In this work we described desorption spectra of carbon monoxide on cobalt foils. Carbon monoxide desorption from cobalt foils was studied in a similar way as prior work, using a mass spectrometric method in an ultra high vacuum system. Two carbon monoxide desorption peaks were observed. These two states correspond to molecular CO and presumably dissociated CO, as it is observed in the case of stepped surfaces of Ni and Co single crystals. An activation energy of around 4.0 kcal/mol is obtained for the molecular state while for the dissociated state the energy is coverage-dependent with a value between 8.0 and 15.0 kcal/mol. The carbon monoxide desorption peaks were fitted with near Gaussian curves which facilitates the analysis of the data to obtain activation energies for desorption. Kinetic parameters for carbon monoxide and hydrogen desorption from nickel and cobalt foils are provided and compared with already published data involving single crystals.

Keywords: Carbon monoxide adsorption; hydrogen adsorption; on nickel and cobalt

1. Introduction

The catalyzed production of hydrocarbons from the hydrogenation of CO has been extensively studied in the last 30 years using modern surface analysis techniques. Although these catalyzed reactions are known since the beginning of this century, it was only in the 70's that Vannice [1] started a systematic study of hydrocarbon production from hydrogen and CO. More recently, Somorjai [2] wrote an excellent review paper on the catalyzed production of C_1 hydrocarbon. Most of the work described in that paper was done with well-characterized surfaces

[1] To whom correspondence should be addressed.

of single crystals. Even though much work has been done on the subject, some questions about the basic steps of these reactions still remain unanswered. For example, in Somorjai's review, he mentions that it is still unclear which surface sites on transition metals dissociate CO.

Most transition metals are good catalysts in the production of hydrocarbons from the reaction of H_2 with CO [1,2]. Intermediate steps for the formation of hydrocarbons are the adsorption and dissociation of both molecular H_2 and CO on the surface of transition metals. Nickel, in particular, is a transition metal which favors the reaction towards the formation of methane, while other transition metals such as iron and cobalt catalyze the formation of higher hydrocarbon molecules [2].

The aim of our studies is to create a bridge of knowledge between basic adsorption studies of these gases on nickel and cobalt single crystals and the industrial processes of syngas production where polycrystalline material is used.

We have pursued a systematic study of CO hydrogenation on polycrystalline surfaces of nickel and cobalt [3–5]. We studied CO methanation reactions on pure Ni and Co powder [3]. Subsequently, we studied in detail the adsorption of H_2 and CO on nickel polycrystalline surfaces [4] and found two states of adsorption for atomic hydrogen. Two states of hydrogen adsorption have been reported in many Ni single crystal studies [5–7], independent of the surface orientation of the substrate. We have more recently studied the adsorption of H_2 on polycrystalline surfaces of cobalt [8] and found also two states of adsorption, as in the case of nickel.

The studies reported here, on the adsorption of CO on cobalt polycrystalline material, have the purpose of completing the whole picture with the hope of obtaining a better understanding of the role of adsorption sites on the end products of the reaction. Therefore, in addition to presenting CO desorption data from cobalt foils, we will make a comparison of results between nickel and cobalt with regard to H_2 and CO adsorption. This comparison is possible since the experiments were performed under identical conditions.

The thermal desorption spectra (TDS) shown in this paper were obtained with a mass spectrometric method.

2. Experimental

2.1. THERMAL DESORPTION FROM THE FOILS USING A MASS SPECTROMETER

We modified a system from AMETEK (Thermox Instruments Division, Pittsburgh, PA) designed for gas analysis. This instrument consists of a vacuum system mounted on a mobile cart which incorporates a Dycor quadrupole gas analyzer. The instrument was equipped with a Balzers 50 ℓ/s turbomolecular pump backed with a Leybold Trivac S/D 1,6 B mechanical pump.

The modification to the instrument included a six-way cross with 2.75 in ConFlat flanges (MDC High Vacuum Components, CA) on top of the turbomolecular

pump. The six-way cross allows us to place a sample manipulator, an Ar ion sputtering gun, the quadrupole mass spectrometer, a Varian variable leak valve and a glass view port on the available flanges. The base pressure of the system after outgassing stayed in the middle 10^{-9} Torr. More details of this system can be found elsewhere [9].

A sample of pure cobalt foil with approximate dimensions of $1.0 \times 1.0 \times 0.01$ cm was cut from a larger piece of foil obtained from Alfa Products, and mounted on the manipulator of an ultrahigh vacuum (UHV) system. The purity of the Co foil was 99.999% pure (Puratronic grade), the highest purity available from Alfa. The Co foil was spotwelded to two 0.09 cm in diameter 316 stainless steel wires which were clamped to 0.32 cm in diameter copper bars. The sample was then resistively heated using a high-current ac power supply. The temperature of the sample was monitored by a 0.013 cm in diameter chromel–alumel thermocouple spot welded to one face of the Co foil.

A Dycor M100M quadrupole mass spectrometer was used to monitor H_2 and CO desorbing from a Co or Ni foil. The desorption spectra can be obtained in a time display mode and stored in the memory of the control unit for later data download to a computer. Typically, four masses are monitored for 120 or 180 s, with a sampling rate of a point every 0.8 s. Real time temperature is recorded using LabTech Notebook software (Laboratory Technologies Corporation, Wilmington, MA). This software coupled with 6B modules from Analog Devices (Norwood, MA), allows acquisition of voltage or current signals with variable sampling rates. The data was transferred to the computer for further analysis and plotting using an appropriate software such as Lotus 123 (Lotus Development Corporation, Cambridge, MA).

2.2. SURFACE ANALYSES

Surface cleanliness and surface elemental composition of the foils were monitored with Auger electron spectroscopy (AES) in an independent vacuum chamber with a base pressure of 1×10^{-9} Torr. AES analyses were performed with a cylindrical mirror analyzer (CMA) from Physical Electronics using 2 keV electrons, 1×10^{-6} A beam current and 2 V peak-to-peak modulation. The spectra were obtained scanning from 15 to 1000 eV energy range. More details of this surface analysis system can be found elsewhere [10].

A surface cleaning recipe for the foils was developed in this chamber. The recipe was followed rigorously in the chamber where the TDS experiments were performed: Once the foils were mounted in the manipulator and introduced inside the vacuum chamber, the foils were flashed to 923 K. AES analyses revealed that the surface was enriched in S after the heating. The foils were then subjected to three cycles of flash desorption to 923 K, in vacuum, and Ar ion sputtering and no more C or S was observed on the surface. A large spot of 1×1 cm was chosen for sputtering and the ion current was maintained constant at 1 μA for 2 min.

2.3. X-RAY DIFFRACTION

X-ray diffraction patterns of the foils were taken at room temperature with a Siemens D5000 diffractometer. The diffraction patterns were obtained with a Cu X-ray tube and a two-circle goniometer in the usual theta–theta geometry. The X-ray tube was operated at 40 keV and 30 mA current, generating mainly Cu K_α radiation of 8.05 keV (0.154 nm). The goniometer was advanced between 40° and 160° at 0.02°/s in the whole 2θ interval. The diffracted X-rays were detected with a solid state detector. The diffraction patterns corresponding to Ni did not show any significant background signal while the diffraction patterns for Co showed visible background as a result of fluorescent scattering.

4. Results and discussion

4.1. DESORPTION OF CO FROM Co FOIL

Before the desorption experiments, the Co foil was cleaned in pure methanol in an ultrasonic bath. Once inside the vacuum chamber, the foil was then subjected to three cycles of flash desorption to 923 K, in vacuum, and Ar ion sputtering for 2 min. Assuming that no more C or S remained on the surface, the foil was then exposed to 100, 500 or 1000 L of CO at 320 K to perform the desorption experiments (1 L = 10^{-6} Torr s). For each exposure, the cleaning cycle was repeated before exposure to CO.

The foil was heated to 923 K, at 5 or 10 K/s, and the desorbing gas detected by the mass spectrometer. Typical desorption spectra obtained from these experiments, using a heating rate of 10 K/s, are displayed in fig. 1. For comparison, similar data of CO desorbing from Ni foil is displayed in fig. 2.

Two CO desorption peaks are observed: a peak around 388 K which presumably corresponds to adsorbed molecular CO, and a peak between 582 and 621 K (depending on the coverage) which presumably corresponds to dissociated CO.

The presence of dissociated CO on the surface of transition metals, when adsorbed at room temperature, is a subject for more discussion. Somorjai [2] has pointed out that dissociation of CO on transition metals occurs at temperatures higher than 400 K. More recently, Papp [11] claimed that dissociative adsorption of CO on Co single crystals above 300 K was observed in his work.

Our data of CO desorption from Ni foil agrees qualitatively well with the work of Goodman, Yates and Madey [12]. Moreover, Lauterbach et al. [13] have demonstrated recently, using FTIRAS techniques, that the desorption peak located at 378 K corresponds to molecular CO adsorption. We can then assume that this is the same in the case of Co foil, since the locations of the peaks are almost identical.

The ratio between adsorbed molecular CO and dissociated CO on Co is inverted

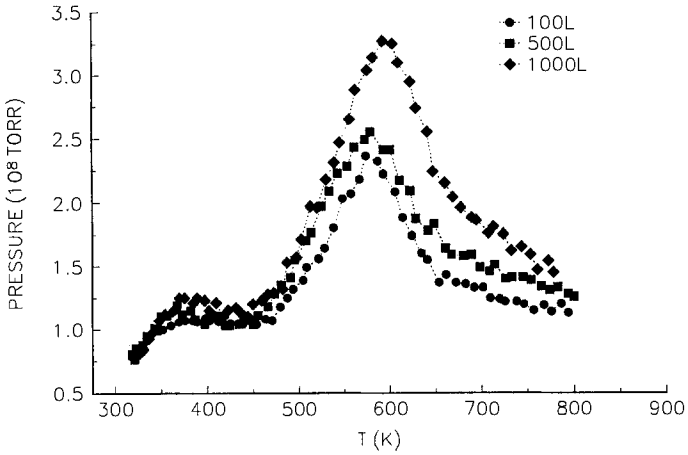

Fig. 1. TDS spectrum of CO desorption from Co foil after exposure to 100, 500 and 1000 L of CO. The heating rate was 10 K/s.

in comparison with the ratio found in the case of Ni (compare figs. 1 and 2). This indicates a greater ability of Co foil to dissociate carbon monoxide than Ni foil. This might be a fundamental difference which would explain why Co catalyzes better the formation of higher hydrocarbon molecules than Ni.

Although this was also concluded from the work of Geerlings et al. [14] using Co single crystals, it was not obvious that the same behavior should have been expected from Co and Ni foils. The CO desorption curve can be fitted with two overlapping curves (each one corresponds to a desorption peak). Individual curves can be described by a general expression of the type

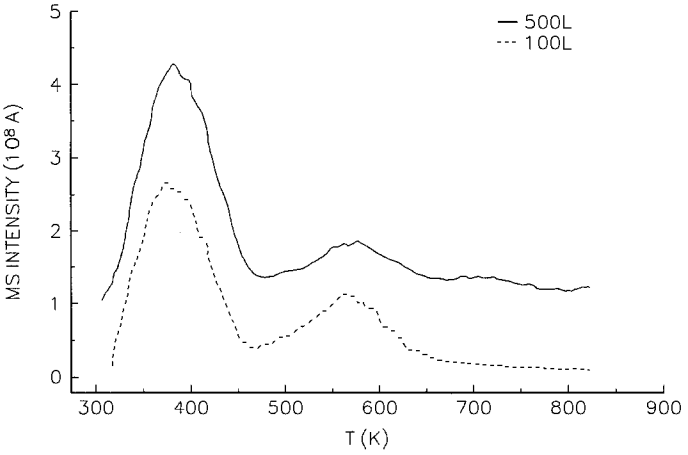

Fig. 2. TDS spectrum of CO desorption from Ni foil after exposure to 100 and 500 L of CO. The heating rate was 12 K/s.

$$I(T) = I_m \exp(-T^2/d^2), \tag{1}$$

where $I(T)$ represents the intensity of the curve at the temperature T, I_m is the intensity at the maximum, and d^2 is related to the width of the bell-shaped curve. Fitted Gaussian curves for a typical CO desorption spectrum, after exposure of the Co foil to 1000 L, are plotted in fig. 3.

Activation energies for desorption for both peaks can be obtained by plotting the rate constant versus the inverse absolute temperature. The rate constant at each temperature point was obtained from the intensity value of the curve and the area integrated up to that temperature point. The fundament of this type of analysis, which agrees well with the more traditional Redhead's method, is given and explained in detail in a previous paper [15]. Activation energies have been rigorously obtained, for the cases of desorption of hydrogen or carbon monoxide from Ni or Co, throughout all these studies in the way described in the next section.

The rate constant (k) is defined in the rate equation for desorption:

$$dN/dt = -kN^n, \tag{2}$$

where dN/dt is the rate of desorption, N is the concentration of adsorbed gas and n is the order of desorption. When molecules dissociate on the surface of transition metals, the order n taken as 2 in the analysis is plausible, but the order n is determined by the best fit of the data to a straight line in an Arrhenius plot. The rate constant k normally obeys an Arrhenius-type rate law of the form

$$k = v_n \exp(-E/RT) \tag{3}$$

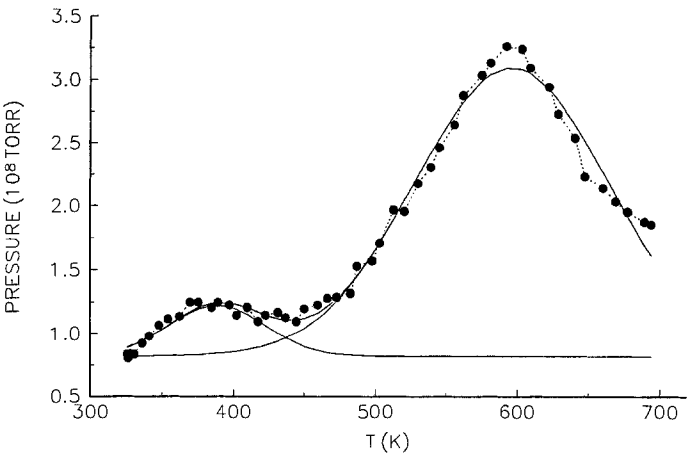

Fig. 3. Same TDS spectrum of CO desorption from Co foil after exposure to 1000 L of CO, heating rate 10 K/s, shown in fig. 1. The data represented with dark circles can also be fitted with two Gaussian curves drawn with solid lines.

where v_n is the pre-exponential factor, R is the gas constant, and E is the activation energy. The constant k was evaluated from the desorption curve using the following relationship:

$$k = A_0^{n-1} B f(T)/[A_0 - A(T)]^n . \tag{4}$$

In eq. (4), A_0 is the total area corresponding to one peak, B is the heating rate, $f(T)$ is the value of the curve at the temperature T, and $A(T)$ is the area under the curve up to the temperature T. The value of A_0 is proportional to the coverage since it represents the initial concentration of atoms adsorbed for a given exposure.

Arrhenius plots for the desorption rate of the two CO peaks shown in fig. 3 are displayed in fig. 4. The activation energies are 4.0 and 8.2 kcal/mol for the first and second peak respectively.

Activation energy for the first peak remained nearly constant (around 4.0 ± 0.5 kcal/mol), with a desorption order $n = 1$, for exposures between 100 and 1000 L. The activation energy for the higher temperature state increased from 8.2 to 15.0 ± 1.0 kcal/mol, as the exposure was decreased from 1000 to 100 L. The desorption order also changed from nearly 2 at 100 L down to 1 for the 1000 L exposure.

The reaction rate can be first order if the desorption of molecular CO is the rate limiting step or if CO gas is formed from two neighboring carbon and oxygen immobile atoms. CO desorption with order 1 and low activation energy should be seen for CO saturated surfaces in lieu of the above argument. An activation energy of 15 kcal/mol is in agreement with the calculated 20 kcal/mol by Papp [11] for dissociative adsorption of CO on Co(1, 1, $\bar{2}$, 0) single crystal.

The orders obtained from this analysis are a clear indication that the first peak

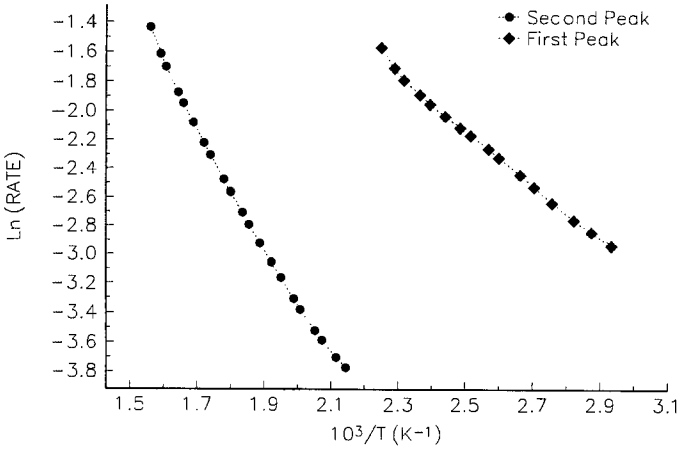

Fig. 4. Plots of CO desorption rate versus inverse absolute temperature for the TDS shown in fig. 3. The slopes correspond to 4.0 kcal/mol for the first desorption peak (◆) and 8.2 kcal/mol for the second desorption peak (●).

corresponds to a first order desorption process while the second peak corresponds to a second order desorption process with coverage-dependent activation energy.

All the kinetic parameters obtained in hydrogen or carbon monoxide desorption from Ni and Co foils, in previous and present work, are summarized in tables 1 and 2. Apparent activation energies for CO-methanation measured in Co and Ni powder are also given in these tables for comparison, since these were the same materials used in the desorption studies. Hydrogen desorption spectra from the respective powders agree well with spectra from the foils. The apparent activation energy for Co powder is lower than the energy from Ni powder and the values agree reasonably well with the CO-methanation activation energy measured on Co single crystals by other researchers [14]. This apparent activation energy for CO-methanation is much lower than the energies reported by Vannice [1] because our experiments were not performed in steady state conditions such as those of his experiments. The only purpose of this methanation study was to compare the reactivity of the Co and Ni powders in which hydrogen desorption experiments were performed.

4.2. X-RAY CHARACTERIZATION OF THE FOILS

The X-ray diffraction data obtained for Co and Ni foils before and after the experiments suggests that the microstructure of the Ni foil changed but the microstructure of the Co foil was unaltered.

Initially, the Ni foil is preferentially oriented in the (1, 1, 0) direction and the Co foil shows preferential orientation in the (1, 0, 1), (0, 0, 2) and (1, 0, 2) directions. After annealing the foils at 900 K in vacuum, the diffraction pattern of Ni is almost identical to the corresponding Ni powder diffraction pattern. There is still some preferential orientation for Ni in the (1, 0, 0) direction (strong line labeled with the Miller index (2, 0, 0)) and the (1, 1, 1) reflexion is somewhat suppressed.

In the case of Co, the structure of the foil does not change much after annealing. Preferential orientation in the (1, 0, 1) and (1, 0, 2) directions remained.

Table 1
Kinetic parameters for desorption from Ni foils. Heating rate, 12 K/s

	Activation energy (kcal/mol)	Order n	Pre-exp. factor (1/s)	T_m (K)
H_2-β_1 state	9.4	1	$1.2\,10^4$	420 [b]
H_2-β_2 state	29.6	2	$2.6\,10^{13}$	480 [b]
CO-molecular state	5.9	1	$6.2\,10^2$	378
CO-dissociat. state	30	2	$2.9\,10^{11}$	570

CO-methanation apparent [a] activation energy 15.7 kcal/mol (ref. [3]), methane start at 423 K [b], 1 atm total pressure.

[a] Not measured in steady state conditions like work reported in ref. [1].
[b] Temperature determined within 10 K error.

Table 2
Kinetic parameters for desorption from Co foils. Heating rate, 10 K/s

	Activation energy (kcal/mol)	Order n	Pre-exp. factor (1/s)	T_m (K)
H_2-β_1 state	4.4	1	65	369
H_2-β_2 state	12.1	2	$9.8\,10^4$	475
CO-molecular state	4.0	1	$\sim 10^2$	388
CO-dissociat. state [a]	15.0	2	$\sim 10^4$	621
	8.0	1		582

CO-methanation apparent [b] activation energy 12.4 kcal/mol (ref. [3]), methane start at 393 K, 1 atm total pressure.

[a] The energy and order for this state depends on the coverage.
[b] Not measured in steady state conditions like in work reported in ref. [1].

Since we do not know what kind of surface changes produce the internal microstructure arrangement in Ni foil, to obtain reproducible desorption results, X-ray characterization suggests that the Ni foil should be annealed before the TDS. Our cleaning procedure in the vacuum chamber already took care of this problem, since the foil was cycled between room temperature and 923 K several times before the TDS was performed.

4.3. RELATIONSHIP BETWEEN ADSORPTION ON ORIENTED SURFACES OF SINGLE CRYSTALS AND POLYCRYSTALLINE SURFACES OF FOILS

4.3.1. Adsorption sites for different crystal surface orientations

Using the program "Surface Architecture and Latuse" [16], we have obtained pictures of the hypothetical surface for an ideal Co (hcp structure) or Ni (fcc structure) crystal with three different orientations: (1, 1, 1), (1, 0, 0) and (1, 1, 0). The numbers correspond to the Miller indexes which define a crystal plane.

There are two possible sites for hydrogen adsorption in any of the three structures. For example, these three surface orientations are represented for Ni in fig. 5. One site is on top of the first Ni atomic layer (site 1), and the other site is on top of the second Ni atomic layer and between Ni atoms of the first layer (site 2). The second type of site would necessarily correspond to adsorption with a larger activation energy, since an adsorbed atom would be coordinated to at least three Ni atoms.

One can notice that the energy for hydrogen adsorption in site 2 is about three times the energy of site 1 in Co or Ni [4,5] (see tables 1 and 2). This is the same ratio of coordination number between site 1 and site 2. These two types of site appear in any of the structures corresponding to different crystal orientations. This would explain the appearance of two H_2 desorption states by TDS, regardless of the surface structure of the Co or Ni crystal.

This explanation could appear naive, knowing that it is well proven [17] that

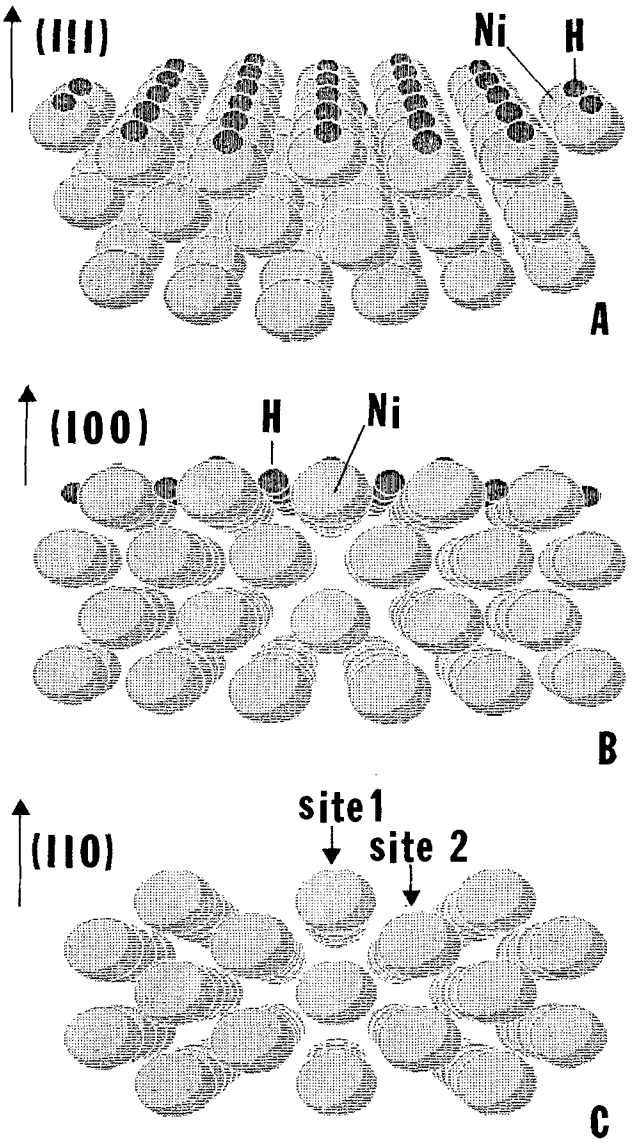

Fig. 5. Pictures of the surface of an ideal Ni single crystal with adsorbed hydrogen atoms for three crystal orientations: (a) (1, 1, 1); (b) (1, 0, 0); and (c) (1, 1, 0). Large spheres correspond to Ni atoms and small dark spheres correspond to hydrogen atoms.

hydrogen adsorbs in two types of three-fold hollow sites (fcc and hcp) on Ni(1, 1, 1), but our argument is that states that are energetically too close in value cannot be resolved by TDS. We probably cannot distinguish by TDS, states coming from on-top-atom sites or bridge-atom sites for hydrogen adsorption.

In the case of Co, the first and second Co atomic layers are almost at the same height, since the crystallographic structure of Co (hcp) is more compacted than the structure of Ni (fcc). These two nearly equivalent adsorption sites will have activation energies not too far apart, as seen in the TDS experiments on hydrogen adsorption [8].

4.3.2. Adsorption sites for polycrystalline surfaces

The crystal planes originating from the Miller indexes, discussed in the previous section, yield the most dissimilar surface structures. A representation of the surface structure of polycrystalline material should be an average of all the possible structures originating from different single crystal orientations. Being these structures the most dissimilar ones, we can assume that the surface structure of polycrystalline material is the combination of the three of them. Thus, hydrogen and CO desorption from Ni and Co foils should show all the desorption peaks observed in experiments performed with crystals involving those orientations.

Hydrogen desorption from Ni single crystals with different surface orientations have always shown two desorption peaks (β_1 and β_2 states) [5–7]. Two peaks of CO desorption were observed from Ni single crystals with stepped surfaces only. The dissociative CO adsorption was preferentially detected when surface steps were present [18].

Similar observations were claimed by Papp with regard to CO adsorption studies on oriented surfaces of Co single crystals [11]. Dissociative adsorption of CO was observed only for open Co surfaces (such as Co$(1, 1, \bar{2}, 0)$), while it was not observed for low index planes.

5. Concluding remarks

Two H_2 desorption states (β_1 and β_2) are observed in Ni and Co powders or foils. These seem to be the same two H_2 states observed in Ni single crystals. The difference in activation energy between these two states in Ni (about 21 kcal/mol) is larger than in Co (about 14 kcal/mol).

Two CO desorption peaks are observed in both cases, for Ni and Co foils. The appearance of the peaks in the temperature scale is very similar (with the same heating rates). A lower temperature peak presumably corresponds to adsorbed molecular CO, and a higher temperature peak presumably corresponds to dissociated CO. The ratio between adsorbed molecular CO and dissociated CO is inverted in Co with relation to the case of Ni. This indicates a greater ability of Co foil to dissociate carbon monoxide than Ni foil. The CO desorption spectra agree well with prior studies involving Ni and Co single crystals with different surface orientations.

Since there are no large differences between Co and Ni foils in their ability to chemisorb hydrogen, the marked difference in CO chemisorption might be funda-

mental in explaining why Co preferentially catalyzes the formation of higher hydrocarbon molecules. Carbon monoxide desorption spectra from Co or Ni polycrystalline material obtained in these studies are almost identical to the desorption spectra from other studies in which stepped surfaces of Ni or Co single crystals were used. This appears to indicate that CO preferentially dissociates on surface steps.

Acknowledgement

We acknowledge Fundación Andes for the donation of equipment used in this research and Pontificia Universidad Católica for providing laboratory space. This research was also partially supported by grants from: the Chilean Government (Fondecyt 0633-91), Universidad Católica (Proyectos DIUC 1993) and a special grant for Latin America provided by the NSF through Fermilab (1993). One of us (ALC) acknowledges critical comments by Keith Hall in the initial part of this work related to hydrogen adsorption by transition metals.

References

[1] M.A. Vannice, J. Catal. 37 (1975) 449.
[2] G.A. Somorjai, Catal. Rev.-Sci. Eng. 23 (1981) 189.
[3] C.A. Luengo, A.L. Cabrera, H.B. MacKay and M.B. Maple, J. Catal. 47 (1977) 1.
[4] A.L. Cabrera, J. Vac. Sci. Technol. A 8 (1990) 3229.
[5] J.N. Russel Jr., S.M. Gates and J.T. Yates Jr., J. Chem. Phys. 85 (1986) 6792.
[6] G. Wedler, G. Fish and H. Papp, Ber. Bunsenges. Phys. Chem. 74 (1970) 186.
[7] K. Christmann, O. Schober, G. Ertl and M. Neumann, J. Chem. Phys. 60 (1974) 4528.
[8] A.L. Cabrera, J. Vac. Sci. Technol. A 11 (1993) 205.
[9] A.L. Cabrera, E. Morales, L. Altamirano and P. Espinoza, Rev. Mex. Fis. 39 (1993) 1099.
[10] A.L. Cabrera, J. Vac. Sci. Technol. A 7 (1989) 2681.
[11] H. Papp, Surf. Sci. 149 (1985) 460.
[12] D.W. Goodman, J.T. Yates Jr. and T.E. Madey, Surf. Sci. 93 (1980) L135.
[13] J. Lauterbach, M. Wittmann and J. Kuppers, Surf. Sci. 279 (1992) 287.
[14] J.J.C. Geerlings, M.C. Zonnevylle and C.P.M. de Groot, Surf. Sci. 241 (1991) 315.
[15] A.L. Cabrera, J. Chem. Phys. 93 (1990) 2854.
[16] M.A. Van Hove and K. Hermann, Surface Architecture and Latuse, A PC-based program, Version 2.0, Lawrence Berkeley Lab., Berkeley, CA (1988).
[17] J.M. MacLaren, J.B. Pendry, P.J. Rous, D.K. Saldin, G.A. Somorjai, M.A. Van Hove and D.D. Vvedensky, *Surface Crystallographic Information Service: A Handbook of Surface Structures* (Reidel, Dordrecht, 1988) p. 327.